Estimating Granger Causality from Fourier and Wavelet Transforms of Time Series Data

Mukeshwar Dhamala,[1] Govindan Rangarajan,[2] and Mingzhou Ding[3]

[1]*Department of Physics and Astronomy, Brains and Behavior Program, Center for Behavioral Neuroscience, Georgia State University, Atlanta, Georgia 30303, USA*

[2]*Department of Mathematics, Indian Institute of Science, Bangalore 560012, India*

[3]*Department of Biomedical Engineering, University of Florida, Gainesville, Florida 33611, USA*

(Received 5 June 2007; published 10 January 2008)

Experiments in many fields of science and engineering yield data in the form of time series. The Fourier and wavelet transform-based nonparametric methods are used widely to study the spectral characteristics of these time series data. Here, we extend the framework of nonparametric spectral methods to include the estimation of Granger causality spectra for assessing directional influences. We illustrate the utility of the proposed methods using synthetic data from network models consisting of interacting dynamical systems.

DOI: 10.1103/PhysRevLett.100.018701 PACS numbers: 05.45.Tp, 02.50.Sk, 02.70.Hm, 45.30.+s

Extracting information flow in networks of coupled dynamical systems from the time series measurements of their activity is of great interest in physical, biological, and social sciences. Such knowledge holds the key to the understanding of phenomena ranging from turbulent fluids to interacting genes and proteins to networks of neural ensembles. Granger causality [1] has emerged in recent years as a leading statistical technique for accomplishing this goal. The definition of Granger causality [1] is based on the theory of linear prediction [2] and its original estimation framework requires autoregressive (AR) modeling of time series data [1,3]. Such parametric Granger causality and associated spectral decompositions have been applied in a wide variety of fields including condensed matter physics [4], neuroscience [5–8], genetics [9], climate science [10,11], and economics [1,12]. However, the parametric modeling methods often encounter difficulties such as uncertainty in model parameters and inability to fit data with complex spectral contents [13]. On the other hand, the Fourier and wavelet transform-based nonparametric spectral methods are known to be free from such difficulties [13] and have been used extensively in the analysis of univariate and multivariate experimental time series [14,15]. A weakness of the current nonparametric framework is that it lacks the ability for estimating Granger causality. In this Letter, we overcome this weakness by proposing a nonparametric approach to estimate Granger causality directly from Fourier and wavelet transforms of data, eliminating the need of explicit AR modeling. Time-domain Granger causality can be obtained by integrating the corresponding spectral representation over frequency [3]. Below, we present the theory and apply it to simulated time series.

Granger causality: The parametric estimation approach.—Granger causality [1] is a measure of causal or directional influence from one time series to another and is based on linear predictions of time series. Consider two simultaneously recorded time series: X_1: $x_1(1), x_1(2), \ldots, x_1(t), \ldots$; X_2: $x_2(1), x_2(2), \ldots, x_2(t), \ldots$ from two stationary stochastic processes (X_1, X_2). Now, using AR representations, we construct bivariate linear prediction models for $x_1(t)$ and $x_2(t)$:

$$x_1(t) = \sum_{j=1}^{\infty} b_{11,j} x_1(t-j) + \sum_{j=1}^{\infty} b_{12,j} x_2(t-j) + \epsilon_{1|2}(t) \quad (1)$$

$$x_2(t) = \sum_{j=1}^{\infty} b_{21,j} x_1(t-j) + \sum_{j=1}^{\infty} b_{22,j} x_2(t-j) + \epsilon_{2|1}(t) \quad (2)$$

along with the univariate models: $x_1(t) = \sum_{j=1}^{\infty} \alpha_j x_1(t-j) + \epsilon_1(t)$ and $x_2(t) = \sum_{j=1}^{\infty} \beta_j x_2(t-j) + \epsilon_2(t)$. Here, ϵ's are the prediction errors. If $\mathrm{var}(\epsilon_{1|2}(t)) < \mathrm{var}(\epsilon_1(t))$ in some suitable statistical sense, then X_2 is said to have a causal influence on X_1. Similarly, if $\mathrm{var}(\epsilon_{2|1}(t)) < \mathrm{var}(\epsilon_2(t))$, then there is a causal influence from X_1 to X_2. These causal influences are quantified in time domain [3] by $F_{j\to i} = \ln \frac{\mathrm{var}(\epsilon_i(t))}{\mathrm{var}(\epsilon_{i|j}(t))}$, where $i = 1, 2$ and $j = 2, 1$.

Experimental processes are often rich in oscillatory content, lending themselves naturally to spectral analysis. The spectral decomposition of Granger's time-domain causality was proposed by Geweke in 1982 [3]. To derive the frequency-domain Granger causality, we start with Eqs. (1) and (2). We rewrite these equations in a matrix form with a lag operator L: $Lx(t) = x(t-1)$ as

$$\begin{pmatrix} b_{11}(L) & b_{12}(L) \\ b_{21}(L) & b_{22}(L) \end{pmatrix} \begin{pmatrix} x_1(t) \\ x_2(t) \end{pmatrix} = \begin{pmatrix} \epsilon_{1|2} \\ \epsilon_{2|1} \end{pmatrix}, \quad (3)$$

where $b_{ij}(L) = \sum_{k=0}^{\infty} b_{ij,k} L^k$ with $b_{ij,0} = \delta_{ij}$ (the Kronecker delta function). The covariance matrix of the noise terms is

$$\mathbf{\Sigma} = \begin{pmatrix} \Sigma_{11} & \Sigma_{12} \\ \Sigma_{21} & \Sigma_{22} \end{pmatrix},$$

where $\Sigma_{11} = \mathrm{var}(\epsilon_{1|2})$, $\Sigma_{12} = \Sigma_{21} = \mathrm{cov}(\epsilon_{1|2}, \epsilon_{2|1})$, and $\Sigma_{22} = \mathrm{var}(\epsilon_{2|1})$. Fourier transforming Eq. (3) yields

$$\begin{pmatrix} B_{11}(f) & B_{12}(f) \\ B_{21}(f) & B_{22}(f) \end{pmatrix} \begin{pmatrix} X_1(f) \\ X_2(f) \end{pmatrix} = \begin{pmatrix} E_1(f) \\ E_2(f) \end{pmatrix}, \tag{4}$$

where the components of the coefficient matrix $[B_{ij}(f)]$ are $B_{lm}(f) = \delta_{lm} - \sum_{k=1}^{\infty} b_{lm,k} e^{-i2\pi fk}$. In terms of transfer function matrix $[\mathbf{H}(f) = [B_{ij}(f)]^{-1}]$, Eq. (4) becomes

$$\begin{pmatrix} X_1(f) \\ X_2(f) \end{pmatrix} = \begin{pmatrix} H_{11}(f) & H_{12}(f) \\ H_{21}(f) & H_{22}(f) \end{pmatrix} \begin{pmatrix} E_1(f) \\ E_2(f) \end{pmatrix}. \tag{5}$$

Then, the spectral density matrix $\mathbf{S}(f)$ is given by

$$\mathbf{S}(f) = \mathbf{H}(f)\Sigma\mathbf{H}^*(f), \tag{6}$$

where * denotes matrix adjoint. To examine the causal influence from X_2 to X_1 one needs to look at the autospectrum of $x_1(t)$ series, which is $S_{11}(f) = H_{11}\Sigma_{11}H_{11}^* + 2\Sigma_{12}\,\mathrm{Re}(H_{11}H_{12}^*) + H_{12}\Sigma_{22}H_{12}^*$. Here, because of the cross terms in this expression for S_{11}, the causal power contribution is not obvious. Geweke [3] introduced a transformation that eliminates the cross terms and makes an intrinsic power term and a causal power term identifiable. For X_1 process, this transformation is achieved by left-multiplying Eq. (4) on both sides with

$$\begin{pmatrix} 1 & 0 \\ -\Sigma_{12}/\Sigma_{11} & 1 \end{pmatrix},$$

which yields

$$\begin{pmatrix} B_{11}(f) & B_{12}(f) \\ \tilde{B}_{21}(f) & \tilde{B}_{22}(f) \end{pmatrix} \begin{pmatrix} X_1(f) \\ X_2(f) \end{pmatrix} = \begin{pmatrix} E_1(f) \\ \tilde{E}_2(f) \end{pmatrix}, \tag{7}$$

where $\tilde{B}_{21}(f) = B_{21}(f) - \frac{\Sigma_{12}}{\Sigma_{11}}B_{11}(f)$, $\tilde{B}_{22}(f) = B_{22}(f) - \frac{\Sigma_{12}}{\Sigma_{11}}B_{12}(f)$, and $\tilde{E}_2(f) = E_2(f) - \frac{\Sigma_{12}}{\Sigma_{11}}E_1(f)$. The elements of the new transfer function $\tilde{\mathbf{H}}(f)$ then become $\tilde{H}_{11}(f) = H_{11}(f) + \frac{\Sigma_{12}}{\Sigma_{11}}H_{12}(f)$, $\tilde{H}_{12}(f) = H_{12}(f)$, $\tilde{H}_{21}(f) = H_{21}(f) + \frac{\Sigma_{12}}{\Sigma_{12}}H_{11}(f)$, and $\tilde{H}_{22}(f) = H_{22}(f)$. Here, $\mathrm{cov}(E_1, \tilde{E}_2) = 0$ and the new variance of $x_2(t)$ is $\tilde{\Sigma}_{22} = \Sigma_{22} - \frac{\Sigma_{12}^2}{\Sigma_{11}}$. Now, the autospectrum of $x_1(t)$ is decomposed into two obvious parts: $S_{11}(f) = \tilde{H}_{11}(f)\Sigma_{11}\tilde{H}_{11}^*(f) + H_{12}(f)\tilde{\Sigma}_{22}H_{12}^*(f)$, where the first term accounts for the intrinsic power of $x_1(t)$ and the second term for causal power due to the influence from X_2 to X_1. Since Granger causality is the natural logarithm of the ratio of total power to intrinsic power [3], causality from X_2 to X_1 (or, 2 to 1) at frequency f is

$$I_{2\to1}(f) = \ln\frac{S_{11}(f)}{S_{11}(f) - (\Sigma_{22} - \frac{\Sigma_{12}^2}{\Sigma_{11}})|H_{12}(f)|^2}, \tag{8}$$

using the expressions for S_{11} and $\tilde{\Sigma}_{22}$ obtained after the transformation. Next, by taking the transformation matrix as

$$\begin{pmatrix} 1 & -\Sigma_{12}/\Sigma_{22} \\ 0 & 1 \end{pmatrix}$$

and performing the same analysis, one can get Granger causality $I_{1\to2}(f)$ from X_1 to X_2, the expression for which can be obtained just by exchanging subscripts 1 and 2 in Eq. (8). Geweke [3] showed that the time-domain measure is theoretically related to the frequency-domain measure as $F_{2\to1} \le \frac{1}{2\pi}\int_{-\pi}^{\pi} I_{2\to1}(f)df$, but for all processes of practical interest the equality holds.

From the above discussion, it is clear that the estimation of frequency-domain Granger causality requires noise covariance and transfer function which are obtained as part of the AR data modeling. The mathematics behind this parametric approach to obtain these quantities is well established. However, for nonparametric methods the current estimation framework does not contain provisions for computing these quantities. Moreover, the parametric estimation method from finite data can often produce erroneous results if the series in Eqs. (1) and (2) are not truncated to proper model orders. There are criteria [16] for choosing proper AR model order, but these criteria cannot always be satisfied. In addition, the AR modeling approach does not always capture all the spectral features [13]. To overcome these difficulties, we propose a nonparametric estimation approach, in which we derive, based on Fourier and wavelet transforms of time series data, noise covariance and transfer function to be used in Geweke's formulas such as Eq. (8) for Granger causality estimates.

Granger causality: The nonparametric estimation approach.—In the nonparametric approach, spectral density matrices are estimated by using direct Fourier and wavelet transforms of time series data. These matrices then undergo spectral density matrix factorization [17,18] and Geweke's variance decomposition [3] for the estimation of Granger causality. To explain this approach, let us consider a bivariate process with time series $x_1(t)$ and $x_2(t)$, their Fourier transforms $X_1(f)$ and $X_2(f)$, and wavelet transforms $W_{X_1}(t, f)$ and $W_{X_2}(t, f)$. Then, the spectral matrix $\mathbf{S}$ is defined as

$$\mathbf{S} = \begin{pmatrix} S_{11} & S_{12} \\ S_{21} & S_{22} \end{pmatrix},$$

where, in the Fourier-based method, $S_{lm} = \langle X_l(f)X_m(f)^*\rangle$, and, in the wavelet method, $S_{lm} = \langle W_{X_l}(t, f)W_{X_m}(t, f)^*\rangle$. Here, $l = 1, 2$, $m = 1, 2$ and $\langle\cdot\rangle$ is averaging over multiple realizations. Smoother Fourier-based spectral density with reduced estimation bias can be obtained by using the multitaper technique [13,19], which involves the use of discrete spheroidal sequences (DPSS) [20]. The continuous wavelet transform $W_{X_l}(t, s)$ at time t and scale s is computed by the convolution of time series x_l with a scaled and translated version of a prototype wavelet $\Psi(\eta)$ that satisfies zero-mean and unity square-norm conditions

[21,22]: $W_{X_l}(t,s) = \frac{1}{\sqrt{s}} \int_{-\infty}^{\infty} d\eta \Psi^*(\frac{\eta - t}{s}) x_l(\eta)$. Using the relationship between s and f for a given prototype wavelet, such as the Morlet wavelet [22,23], one can transform $W_{X_l}(t,s)$ into $W_{X_l}(t,f)$. The wavelet transform at $f = 0$ can be obtained by a numerical extrapolation. $\mathbf{S}(f)$ or $\mathbf{S}(t,f)$ thus formed is a square matrix that can be defined in the interval $[-\pi, \pi]$ and, for all processes of practical interest, satisfies the following properties: (i) $S(\theta)$ is Hermitian, non-negative, and $S(-\theta) = S^T(\theta)$, where $\theta = 2\pi f$ and T denotes matrix transpose, and (ii) $S(\theta)$ is integrable and has a Fourier series expansion, $S(\theta) = \sum_{k=-\infty}^{\infty} \gamma_k e^{ik\theta}$, where the covariance sequence $\{\gamma_k\}_{-\infty}^{\infty}$ is formed by $\gamma_k = (1/2\pi) \int_{-\pi}^{\pi} S(\theta) e^{-ik\theta} d\theta$.

According to the factorization theorem [17,24], the spectral density matrix $\mathbf{S}$ as defined above can be factored [25] into a set of unique minimum-phase functions:

$$\mathbf{S} = \psi \psi^*, \tag{9}$$

where * denotes matrix adjoint, $\psi(e^{i\theta}) = \sum_{k=0}^{\infty} \mathbf{A}_k e^{ik\theta}$ is defined on the unit circle $\{|z| = 1\}$, and $\mathbf{A}_k = (1/2\pi) \times \int_{-\pi}^{\pi} \psi(e^{i\theta}) e^{-ik\theta} d\theta$. Moreover, ψ can be holomorphically extended [25] to the inner disk $\{|z| < 1\}$ as $\psi(z) = \sum_{k=0}^{\infty} A_k z^k$, where $\psi(0) = \mathbf{A}_0$, a real, upper triangular matrix with positive diagonal elements. Similarly, S and H can be defined as functions of z with $H(0) = I$. Comparing the right-hand sides of Eqs. (6) and (9) at $z = 0$ we get

$$\Sigma = \mathbf{A}_0 \mathbf{A}_0^T. \tag{10}$$

Rewriting Eq. (9) as $\mathbf{S} = \psi \mathbf{A_0^{-1}} \mathbf{A_0} \mathbf{A^T} \mathbf{A_0^{-T}} \psi^*$ and comparing with Eqs. (6) and (10), we arrive at the expression for the transfer function:

$$\mathbf{H} = \psi A_0^{-1}. \tag{11}$$

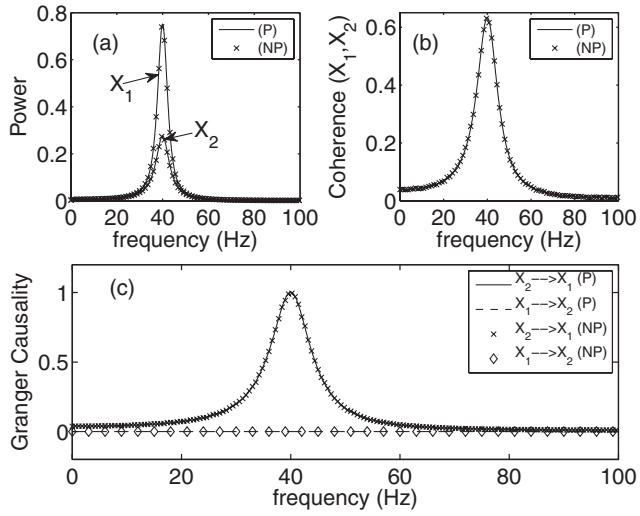

FIG. 1. (a) Power, (b) coherence, and (c) Granger causality spectra from both Fourier transform-based nonparametric (NP) and parametric (P) methods. There is an excellent agreement between NP and P estimates.

Now, by substituting the specific elements of the noise covariance and transfer function from Eqs. (10) and (11) into Eq. (8), one can estimate pairwise Granger causality spectra. In the case of the wavelet, these calculations are repeated along the time axis for each time point to get the time-frequency representation of Granger causality.

Numerical examples.—We consider network models with two autoregressive processes X_1 and X_2 as nodes where $X_1(t) = 0.55X_1(t-1) - 0.8X_1(t-2) + C(t)X_2(t-1) + \epsilon(t)$ and $X_2(t) = 0.55X_2(t-1) - 0.8X_2(t-2) + \xi(t)$. Here, t is a time index, $\epsilon(t)$ and $\xi(t)$ are independent white noise processes with zero means and unit variances, $C(t)$ is the coupling strength, and the sampling rate is considered to be 200 Hz. By construction, only X_2 has a causal influence on X_1. First, we fix $C(t)$ at 0.2 $\forall$ t, generate a data set of 5000 realizations (trials), each consisting of 5000 data points, and apply the Fourier-based nonparametric method. The power spectra of X_1 and X_2 [Fig. 1(a)] and coherence spectra between X_1 and X_2 [Fig. 1(b)] show 40 Hz peaks. Figure 1(c) shows the Granger causality spectra. Here, both the nonparametric (NP) and parametric (P) approaches yield identical results, recovering correctly the underlying directional influences. Since the proper model order is chosen here and the data set is large, the parametric causality estimates can be assumed to represent the theoretical values. Next, we let the unidirectional coupling of X_2 to X_1 change in its strength $C(t)$ over time as shown in Fig. 2(a), generate 5000 realizations, each with

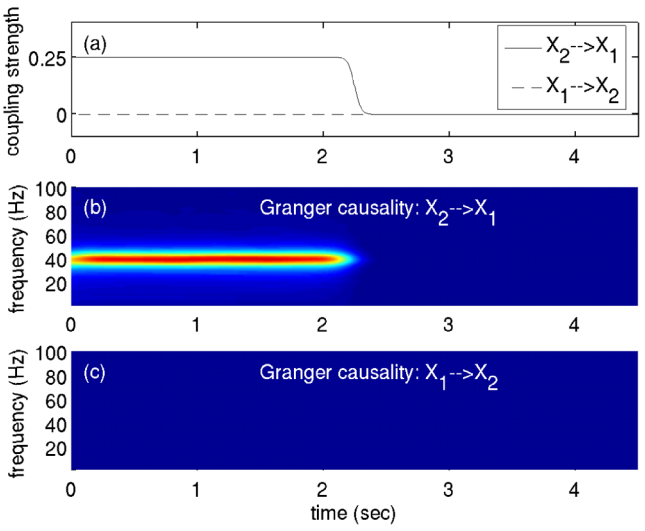

FIG. 2 (color online). Wavelet-based Granger causality: time-frequency representation of causality. (a) Temporal structures of couplings constructed in the network model: the coupling of X_2 with X_1 stays 0.25 during time $[0, 2]$ sec, slowly changes to 0 during $[2, 2.25]$ sec, and stays 0 during time >2.25 sec, whereas the coupling of X_1 with X_2 is 0 throughout. The slow transition in the middle is modeled by the tangent of a hyperbolic function. (b),(c) Time-frequency maps of Granger causality correctly represent the temporal structures of couplings as in (a) for the network model.

900 time points. Then, the wavelet spectra are computed for all the trials using the Morlet wavelet (as used in [22]). The average wavelet spectra are obtained by averaging over these individual spectra. The average spectra at a time point is subsequently factored, and $\mathbf{H}$ and Σ are obtained and used in Eq. (8) to obtain Granger causality spectra. By repeating these calculations along time axis, one gets the complete time-frequency maps of Granger causality [Figs. 2(b) and 2(c)], which also recovers the correct directional influences. Granger causality magnitude increases with coupling strength.

Here, the proposed Granger causality techniques are tested on data sets with a large number of long trials. However, these techniques can also be used reliably with fewer trials. Increasing the number of trials leads to spectral estimates with smaller variance. A single, sufficiently long stationary time series can be broken into smaller segments, each of which can be treated as a distinct trial. The use of multitaper [13] and multiwavelet [26] techniques can yield better estimates of Granger causality in the case of a data set with shorter length and fewer trials. See the supplementary material [27] for additional numerical examples and applications to brain signals.

Conclusion.—Granger causality is a key technique for assessing causal relations and information flow among simultaneous time series. Its traditional parametric estimation framework often suffers from uncertainty in model order selection and inability to fully account for complex spectral features. We develop a nonparametric approach based on the direct Fourier and wavelet transforms of data that eliminates the need of parametric data modeling and extends the capability of Fourier and wavelet-based suites of nonparametric spectral tools. It is expected that the integration of the proposed method into existing laboratory analysis routines will provide the basis for gaining deeper insights into the organization of dynamical networks arising in many fields of science and engineering [28].

We thank G. T. Wilson for useful communications. This work was supported by NIH Grant No. MH71620. G. R. was also supported by grants from DRDO, DST (No. SR/S4/MS:419/07) and UGC (under SAP-Phase IV).

[1] C. W. J. Granger, Econometrica **37**, 424 (1969).
[2] N. Wiener, in *Modern Mathematics for the Engineer*, edited by E. F. Beckenbach (McGraw-Hill, New York, 1949).
[3] J. Geweke, J. Am. Stat. Assoc. **77**, 304 (1982).
[4] R. Ganapathy, G. Rangarajan, and A. K. Sood, Phys. Rev. E **75**, 016211 (2007).
[5] M. J. Kaminski, M. Ding, W. A. Truccolo, and S. L. Bressler, Biol. Cybern. **84**, 463 (2001).
[6] A. Brovelli, M. Ding, A. Ledberg, Y. Chen, R. Nakamura, and S. L. Bressler, Proc. Natl. Acad. Sci. U.S.A. **101**, 9849 (2004).
[7] R. Goebel, A. Roebroeck, D. S. Kim, and E. Formisano, Magn. Reson. Imaging **21**, 1251 (2003).
[8] A. K. Seth and G. M. Edelman, Neural Comput. **19**, 910 (2007).
[9] N. D. Mukhopadhyay and S. Chatterjee, Bioinformatics **23**, 442 (2006).
[10] R. K. Kaufmann and D. I. Stern, Nature (London) **388**, 39 (1997).
[11] T. J. Mosedale, D. B. Stephenson, M. Collins, and T. C. Mills, J. Clim. **19**, 1182 (2006).
[12] C. Hiemstra and J. D. Jones, J. Finance **49**, 1639 (1994).
[13] P. P. Mitra and B. Pesaran, Biophys. J. **76**, 691 (1999).
[14] G. M. Jenkins and D. G. Watts, *Spectral Analysis and its Applications* (Holden-Day, San Francisco, 1968); D. Percival and A. Walden, *Spectral Analysis for Physical Applications: Multivariate and Conventional Univariate Techniques* (Cambridge University Press, Cambridge, England, 1993).
[15] D. Percival and A. Walden, *Wavelet Methods for Time Series Analysis* (Cambridge University Press, Cambridge, UK, 2000).
[16] H. Akaike, IEEE Trans. Autom. Control **19**, 716 (1974); G. Schwarz, Ann. Stat. **6**, 461 (1978).
[17] G. T. Wilson, SIAM J. Appl. Math. **23**, 420 (1972); J. Multivariate Anal. **8**, 222 (1978).
[18] A. H. Sayed and T. Kailath, Numer. Linear Algebra Appl. **8**, 467 (2001).
[19] D. J. Thomson, Proc. IEEE **70**, 1055 (1982).
[20] D. Slepian and H. O. Pollak, Bell Syst. Tech. J. **40**, 43 (1961), part I.
[21] I. Daubechies, IEEE Trans. Inf. Theory **36**, 961 (1990).
[22] C. Torrence and G. Compo, Bull. Am. Meteorol. Soc. **79**, 61 (1998).
[23] P. Goupillaud, A. Grossman, and J. Morlet, Geoexploration **23**, 85 (1984).
[24] P. Masani, in *Multivariate Analysis*, edited by P. R. Krishnaiah (Academic, New York, 1966), p. 351.
[25] Wilson algorithm [17] seeks an iterative solution to the m-dimensional problem: $\psi(e^{i\theta})\psi(e^{i\theta})^* - \mathbf{S}(\theta) = 0$; $-\pi \le \theta \le \pi$. Linearizing the problem and denoting successive iterates by subscript n, we obtain $\psi_{n+1}\psi_n^* + \psi_n\psi_{n+1}^* = \mathbf{S} + \psi_n\psi_n^*$, which becomes $\psi_{n+1} = \psi_n\{[\psi_n^{-1}\mathbf{S}\psi_n^{-1*} + \mathbf{I}]^+ + \mathbf{R}_n\}$, where $\mathbf{R}_n$ satisfies $\mathbf{R}_n + \mathbf{R}_n^* = 0$, and $[\cdot]^+$ operator is defined as $[g]^+ = \beta_0/2 + \sum_{k=1}^{\infty}\beta_k \exp(ik\theta)$ provided $g = \sum_{k=-\infty}^{\infty}\beta_k \exp(ik\theta)$. It is guaranteed [17] that ψ_n converges to ψ.
[26] J.-S. Brittain, D. M. Halliday, B. A. Conway, and J. B. Nielsen, IEEE Trans. Biomed. Eng. **54**, 854 (2007).
[27] See EPAPS Document No. E-PRLTAO-99-026753 for (i) additional numerical examples and (ii) application to brain signals. For more information on EPAPS, see http://www.aip.org/pubservs/epaps.html.
[28] T. Schreiber, Phys. Rev. Lett. **85**, 461 (2000); M. G. Rosenblum and A. S. Pikovsky, Phys. Rev. E **64**, 045202 (2001); L. Lee, K. Friston, and B. Horwitz, NeuroImage **30**, 1243 (2006); A. R. McIntosh and F. Gonzalez-Lima, Hum. Brain Mapp. **2**, 2 (1994); L. Zhu, Y.-C. Lai, F. Hoppensteadt, and J. He, Neural Comput. **15**, 2359 (2003).